PHYSICAL REVIEW B **67**, 140508(R) (2003)

# Nonequilibrium order-disorder vortex transitions in $Bi_2Sr_2CaCu_2O_{8+\delta}$

B. Kalisky, D. Giller, A. Shaulov, and Y. Yeshurun
*Institute of Superconductivity, Bar-Ilan University, Ramat-Gan 52900, Israel*
(Received 26 December 2002; published 29 April 2003)

Magneto-optical snapshots of the induction distribution across a $Bi_2Sr_2CaCu_2O_{8+\delta}$ crystal subjected to ramped magnetic fields reveal strong effects of transient disordered vortex states near the disorder-driven vortex phase transition. These transient states, predominantly generated by edge contamination during field ascending and by supercooling of the disordered vortex lattice during field descending, cause smearing of the transition and shift of its onset towards lower inductions. With decreasing temperature, these effects are more pronounced as the lifetime of the transient vortex states increases. Similar effects are observed with increasing field sweep rates, as transient states with shorter lifetime play a role. These observations clarify previously reported puzzles, e.g., the absence of the second magnetization peak at low temperatures, its appearance at longer times, and the shift of its onset to lower inductions for higher field sweeping rates.

DOI: 10.1103/PhysRevB.67.140508 PACS number(s): 74.25.Qt, 64.60.My, 74.72.Hs

The nature of the disorder-driven solid-solid vortex phase transition in high-temperature superconductors has been an intriguing issue in physics of the vortex matter.[1–4] Various experiments indicated the first-order nature of this transition; these include vortex dithering,[3] history dependent magnetic measurements,[5] and ''supercooling'' experiments,[6,7] demonstrating quenching of the disordered vortex phase by rapid decrease of the field. The results of these experiments have led to the common view of the solid-solid transition line as an extension of the first-order melting line.[3,6] However, along this ''unified'' order-disorder transition line, the magnetic signature of the transition varies considerably; while the melting transition is manifested by a sharp jump in the reversible magnetization, the solid-solid transition is manifested by the onset of a second magnetization peak (''fishtail''), which is gradually smeared as temperature is lowered until, below a certain temperature, it disappears altogether.[1,8] Consequently, the measured transition line terminates at a certain point, leading to peculiarities of unidentified physical origin in the vortex matter phase diagram.[9,10] In this paper we employ time resolved magneto-optical technique to demonstrate that in magnetic measurements the thermodynamic solid-solid vortex phase transition is inevitably obscured by nonequilibrium order-disorder transitions involving transient disordered vortex states. The lifetime of these transient states plays a key role in shaping the magnetization curves near the solid-solid vortex phase transition. It increases monotonically with the induction $B$, exhibiting a sharp increase in close vicinity of the thermodynamic transition induction $B_{od}$.[11,12] We measure the lifetime spectrum of the transient states in $Bi_2Sr_2CaCu_2O_{8+\delta}$ (BSCCO)and show that its variations with temperature explain a line of previously reported puzzling results, e.g., smearing of the fishtail and its disappearance at low temperatures, development of the fishtail with time at low temperatures, and the shift of its onset to lower inductions for higher field sweeping rates.

Measurements were performed on a $1.55\times1.25\times0.05$-$mm^3$ BSCCO single crystal with $T_c=92$ K (optimally doped), at different temperatures between 18 and 30 K. The crystal was grown using the traveling solvent floating zone method.[13] This crystal was specially selected for its uniformity of flux penetration and was checked by magneto-optical imaging before and after it was cut into a rectangle. A magneto-optical image of the crystal taken at $T=23$ K and applied field of 550 G is shown in the inset to Fig. 1. The straight line indicates the location where the induction profiles were taken. Two types of experiments were performed. In the first one, referred to as field sweep up (FSU) experiment, the sample was cooled down to the measuring temperature in zero field, then the external magnetic field, $H_{ext}$, was ramped up from zero to about 850 G, well above the order-disorder transition field $B_{od}$, at a constant rate between 4 and 1600 G/sec. In the second type of experiments, referred to as field sweep down (FSD) experiment, an external field of 850 G was applied for long enough time to ensure establishment of a disordered vortex state. The field was then

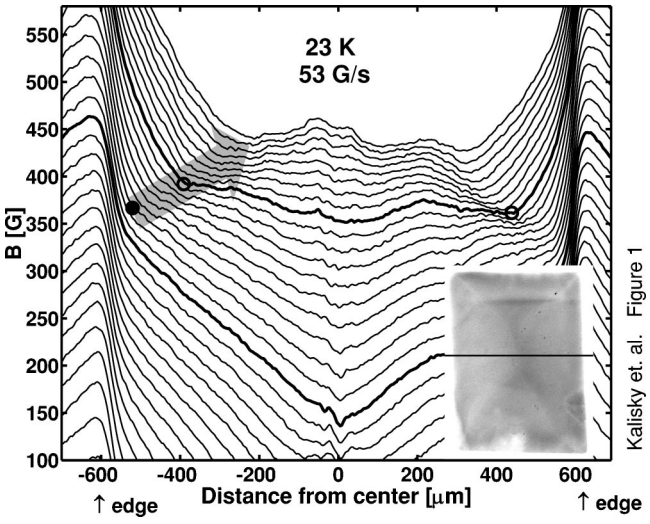


FIG. 1. Induction profiles in BSCCO at $T=23$ K, measured during field sweep up (FSU) experiment at a rate of 53 G/s. The bold lines indicate two typical profiles: smooth profile for $H_{ext}=410$ G and profile with breaks (marked by open circles) for $H_{ext}=620$ G. The bold circle marks the first break at $B_{f0}=370$ G for $H_{ext}=430$. The gray arrow indicates direction of movement of the break. Inset: typical magneto-optical image of the BSCCO sample taken at 23 K with applied field of 550 G.

 

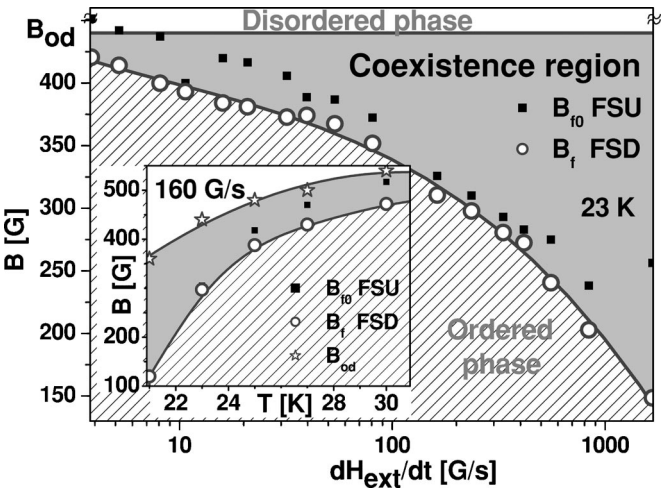


FIG. 2. Variations of the inductions $B_{f0}$ (squares) and $B_f$ (circles) with field sweep rate at $T=23$ K. The dashed line is the estimated $B_{od}$. The dashed and clear areas indicate quasiordered and disordered vortex phases, respectively. The gray area indicates the coexistence region of quasiordered and transient disordered states. Inset: temperature dependence of $B_{od}$ (stars), $B_{f0}$ (squares), and $B_f$ (circles) measured at constant field sweep of 160 G/s.

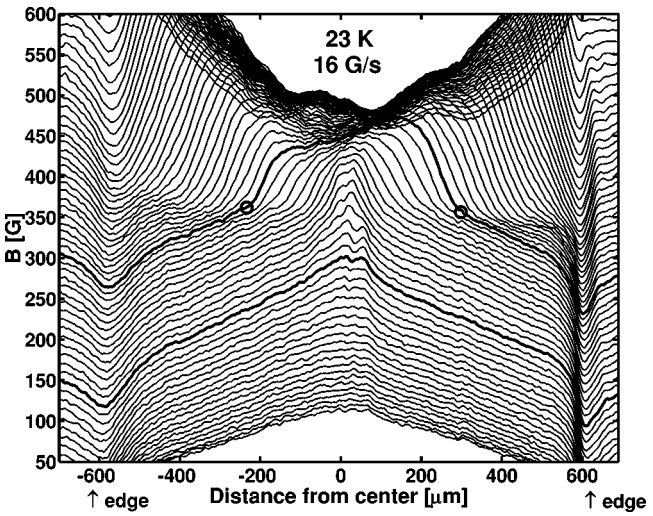


FIG. 3. Induction profiles in BSCCO at $T=23$ K, measured during field sweep down (FSD) experiment at a rate of 16 G/s. The bold lines are two typical profiles: smooth profile and profile with breaks (marked by circles).

ramped down to zero at a constant rate between 4 and 1600 G/sec. While the external magnetic field was ramped (up or down), snapshots of the induction distribution across the crystal surface were taken successively using iron-garnet indicators with in-plane anisotropy[14] and a high speed charge-coupled device (CCD) video camera with exposure time of 36 ms. For rates smaller than 300 G/s snapshots were taken at a constant field intervals of 10 G. For faster rates, snapshots were taken every 36 ms.

Figure 1 shows the induction profiles across the crystal width deduced from the magneto-optical images, taken at $T=23$ K, while the external field was ramped up at a rate of 53 G/sec. When $H_{ext}$ reaches a value of approximately 430 G, a sharp change in the slope of the profile (''break'') appears at $B_{f0}\approx 370$ G, indicating coexistence of two distinct vortex phases characterized by high and low persistent current densities: a high persistent current state near the sample edges and a low persistent current state near the center.[12] When the external field is further increased, the break moves towards the sample center, while the induction at the break monotonically increases. Increasing sweeping rate, or decreasing temperature, shifts $B_{f0}$ downwards, widening the range of external magnetic fields for which the coexisting states are observed. The effects of sweep rate and temperature on $B_{f0}$ are described by the squares in Fig. 2 and its inset, respectively.

Apparently different results were obtained in field sweep down experiments. Figure 3 shows the induction profiles taken at $T=23$ K, while the external field was ramped down at a rate of 16 G/sec. For external fields between 420 and 240 G the profiles exhibit a break, progressing into the sample interior with time. In contrast to the FSU experiments, here the breaks appear at the same induction, $B_f=360$ G, independent of the location in the sample. As above, the breaks reveal coexistence of low and high persistent current states, near the sample edge and in the sample interior, respectively. The value of $B_f$ is strongly suppressed by increasing the sweep rate or decreasing temperature, exhibiting similar behavior to that of $B_{f0}$, as depicted in Fig. 2 (circles).

Obviously, the breaks in the induction profiles observed in the FSU and FSD experiments do not signify the thermodynamic order-disorder vortex phase transition, since the induction value at the break depends on the rate of change of the external field. Moreover, in FSU experiments, it depends also on time and location in the sample. We therefore interpret the break as signifying coexistence of transient disordered state and a quasiordered state.[7,12] The origin of the transient disordered state is different in FSU and FSD experiments, giving rise to the different results obtained in these two types of experiments (see Figs. 1 and 3). However, as we show below, both experiments point to the same underlying physics.

In FSU experiments, vortices are continuously injected into the sample through an inhomogeneous surface barrier,[11,12,15,16] creating a transient disordered state near the sample edges. At the same time annealing of the injected transient states takes place. As proposed by Paltiel *et al.*,[11] this transient state anneals during a characteristic lifetime $\tau$, which is relatively short for $B \ll B_{od}$ and diverges as $B$ approaches $B_{od}$.[12] For inductions far below $B_{od}$, $\tau$ is too short to be detected, thus the profiles appear smooth, without a break (the sharp induction step at the edges is due to surface currents[17]). The break appears for the first time when the lifetime of the injected transient state is long enough to generate a detectable magneto-optical signal. This occurs when $\tau(dB/dt)=\Delta B$, where $\tau(dB/dt)$ represents the induction change due to injection of transient disordered state during its lifetime $\tau$, and $\Delta B$ is the experimental induction resolution ($\sim 1$ G in our system). This first detectable transient state generates a large induction slope near the edges, merging with the induction profile of the quasiordered state inside the sample, creating a ''break'' in the profile at $B_{f0}$. As the external field is further increased, the lifetime of the injected

transient state increases, and as a result, it penetrates deeper into the sample.[11,12] Consequently, the break progresses toward the sample center and the induction $B_f$ at the break increases towards $B_{od}$.

As the external field sweep rate increases, the first appearance of the break is shifted down to lower inductions, as $\tau(dB/dt)=\Delta B$ is fulfilled for transient disordered states with smaller lifetime. Consequently, the coexistence induction range, $\Delta B_{coex}=B_{od}-B_{f0}$, increases, as shown in Fig. 2. This range can also be increased, for a constant sweep rate, by lowering the temperature, because $\tau$ increases as temperature decreases, as demonstrated in the inset to Fig. 2. As a result of increasing $\tau(B)$ with lowering temperature, the equation $\tau(B)=1/(dB/dt)$ is fulfilled for a lower induction $B_{f0}$ and the coexistence range becomes wider.

Although the results of FSD experiments are apparently different from those of FSU, they lead to the same conclusions. As mentioned above, the break in the profiles in the FSD experiments has the same meaning as in FSU experiments. However, the origin of the transient disordered state in FSD experiments is different; it results from ''supercooling'' of the disordered vortex lattice.[6] The initial state of the vortices in the FSD experiments is a thermodynamic disordered state. As the field is rapidly lowered below the transition field, this disordered state is supercooled to inductions below $B_{od}$ and consequently the apparent solid-solid transition $B_f$ shifts below $B_{od}$. Larger sweep-rates induce ''deeper'' supercooling, shifting $B_f$ further down.[18] As $B_{od}$ is crossed while ramping the field down, transient disordered states with the same spectrum of lifetimes $\tau(B)$ are generated everywhere, independent of the location. For a given sweep rate, $B_f$ is recorded when the lifetime $\tau$ at $B_f$ equals the time resolution of the experiment, i.e., $\tau(dB/dt)=\Delta B$. Thus $B_f$ is independent of location as observed experimentally. Since $\tau$ increases monotonically as $B_{od}$ is approached, the relation $\tau(dB/dt)=\Delta B$ indicates that $B_f$ is reduced as $dB/dt$ increases, also consistent with the experiment. It should be noted that $B_f$ in FSD experiments has the same meaning as $B_{f0}$ in FSU experiments, as both are related to the transient state with the shortest detectable lifetime. This is demonstrated in Fig. 2, which shows that both $B_f$ and $B_{f0}$ have approximately the same value and the same dependence on temperature and field sweep rate.

The dependence of $\tau$ on $B$ can be determined from our experiment, as the knowledge of $\Delta B/(dB/dt)$ determines $\tau$ at $B_f$. This is shown in Fig. 4 for temperatures 21–30 K.[19] Evidently, $\tau$ increases monotonically with $B$; it depends weakly on $B$ far below $B_{od}$ and increases sharply as $B_{od}$ is approached. Clearly, the lifetime of the transient disordered state should diverge in close vicinity of $B_{od}$, since the disordered state is thermodynamically favored as $B_{od}$ is crossed.[11,12] Thus the data of Fig. 4 may be used to estimate the true value of the thermodynamic transition induction $B_{od}$ by fitting the data to $\tau_0/(1-B/B_{od})$ in the close vicinity of $B_{od}$[20]. Estimated values of $B_{od}(T)$ are marked by stars in the inset to Fig. 2.

The above observations clarify several previously reported puzzles. In particular, we argue that the absence of the

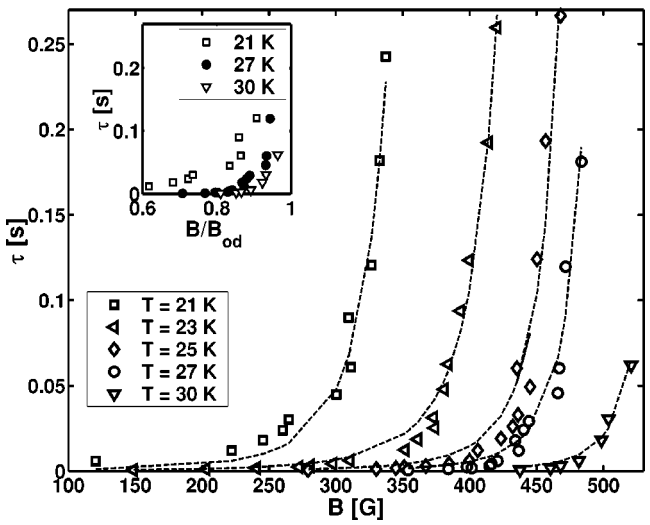


FIG. 4. Lifetime spectra $\tau(B)$ of transient disordered states at the indicated temperatures. Dashed lines are guides to the eye. Inset: lifetime $\tau$ as a function of scaled induction $B/B_{od}$ for $T=21$, 27, and 30 K.

fishtail at low temperatures,[8] its appearance at longer times,[8,21,22] and the shift of its onset to higher inductions as time evolves,[22] can be traced to the appearance of transient states with a lifetime spectrum $\tau(B)$. The induction $B_{f0}$ corresponding to the first appearing break (or equivalently $B_f$) is of prime importance as it signals the onset of the fishtail in local magnetization curves, $M_{local}=B_{local}-H_{ext}$ vs $B_{local}$, everywhere in the sample.[23] Obviously, $B_{f0}$ also signifies the onset of the fishtail in the conventional, global magnetization measurements. The induction range for which a break in the profiles occurs determines the sharpness of the fishtail in global measurements. Thus, from the data of Fig. 2, the fishtail smearing with temperature decrease or field sweeping rate increase is clearly expected. Moreover, below a certain temperature the fishtail may disappear altogether as $B_{f0}$ is shifted to extremely low fields. In this temperature range, the lifetime of the transient disordered states are long enough to enable the transient state to penetrate into the entire sample without annealing. Obviously, as the sweep rate is decreased (time window is expanded), transient states relax and the fishtail emerges. The fishtail onset, being related to $B_{f0}$, is shifted with time to higher inductions as $B_{f0}$ increases towards $B_{od}$.

One reaches the same conclusions considering the lifetime spectrum $\tau(B)$ of the transient disordered states. The inset to Fig. 4 shows the ''scaled'' $\tau(B)$ for $T=21$, 27, and 30 K. Evidently, the lifetime spectrum widens as the temperature is lowered, i.e., for a constant $(B-B_{od})$ the lifetime of the transient state increases with the decrease of temperature. As a result, the fishtail onset is smeared as temperature is lowered and the measured thermodynamic solid-solid phase transition is obscured, until at low enough temperatures it disappears altogether. As the transient states relax the fishtail appears. The transient states at lower fields anneal faster, thus the onset of the fishtail shifts to higher induction with time, approaching $B_{od}$, and, concurrently, the fishtail sharpens.

In conclusion, our time resolved magneto-optical measurements reveal the key role played by transient vortex states and their lifetime spectrum on the vortex solid-solid phase transition. The transient vortex states give rise to nonequilibrium order-disorder vortex transition, obscuring the thermodynamic transition. This effect is especially pronounced at low temperatures, impeding measurements of the thermodynamic transition induction at low temperatures in conventional time windows. This explains the apparent termination of the measured order-disorder transition line at a finite temperature. The effect is also pronounced at short times, or high magnetic field sweep rates, giving rise to strong dynamic effects near the transition. These observations may also explain the influence of defects on broadening the fishtail onset; defects give rise to metastable disordered vortex states with increased lifetime. Thus the lifetime spectrum of the transient vortex states is sample dependent as will be described elsewhere.

This manuscript is a part of B.K.'s Ph.D. thesis. We thank Y. Wolfus and E. Zeldov for many helpful discussions, and T. Tamegai for providing us with the $Bi_2Sr_2CaCu_2O_{8+\delta}$ crystal. A.S. acknowledges support from the Israel Science Foundation (ISF). Y.Y. acknowledges support from the ISF Center of Excellence Program, and by the Heinrich Hertz Minerva Center for High Temperature Superconductivity.

[1] B. Khaykovich *et al.*, Phys. Rev. Lett. **76**, 2555 (1996).
[2] R. Cubitt *et al.*, Nature (London) **365**, 407 (1993); S. L. Lee *et al.*, Phys. Rev. Lett. **71**, 3862 (1993).
[3] N. Avraham *et al.*, Nature (London) **411**, 451 (2001).
[4] D. Giller *et al.*, Phys. Rev. B **60**, 106 (1999); Y. Radzyner, A. Shaulov, and Y. Yeshurun, *ibid.* **65**, 100513(R) (2002).
[5] S. B. Roy and P. Chaddah, Physica C **279**, 70 (1997); S. Kokkaliaris *et al.*, Phys. Rev. Lett. **82**, 5116 (1999); Y. Radzyner *et al.*, Phys. Rev. B **61**, 14 362 (2000).
[6] C. J. van der Beek *et al.*, Phys. Rev. Lett. **84**, 4196 (2000).
[7] D. Giller *et al.*, Physica C **341**, 987 (2000).
[8] Y. Yeshurun *et al.*, Phys. Rev. B **49**, R1548 (1994).
[9] M. F. Goffman *et al.*, Phys. Rev. B **57**, 3663 (1998); V. F. Correa *et al.*, *ibid.* **63**, 092502 (1998).
[10] S. Li and H. Wen, Phys. Rev. B **65**, 214515 (2002).
[11] Y. Paltiel *et al.*, Nature (London) **403**, 398 (2000); Phys. Rev. Lett. **85**, 3712 (2000).
[12] D. Giller *et al.*, Phys. Rev. Lett. **84**, 3698 (2000).
[13] N. Motohira *et al.*, J. Ceram. Soc. Jpn. **97**, 994 (1989).
[14] V. K. Vlasko-Vlasov *et al.*, in *Physics and Materials Science of Vortex States, Flux Pinning and Dynamics*, *NATO Advanced Study Institute, Series E: Applied Sciences*, edited by R. Kossowsky *et al.* (Kluwer, Dordrecht, 1999), Vol. 356, p. 205.
[15] C. P. Bean and J. D. Livingston, Phys. Rev. Lett. **12**, 14 (1964).
[16] L. Burlachkov, Phys. Rev. B **47**, 8056 (1993).
[17] M. V. Indenbom *et al.*, Physica C **222**, 203 (1994).
[18] H. Kupfer *et al.*, Phys. Rev. B **63**, 214521 (2001).
[19] In calculating $\tau$ we approximated $dB/dt$ by $dH_{ext}/dt$. This is justified when relaxation effects may be neglected, i.e., for high sweep rates and low temperatures.
[20] This approximation is the first nonvanishing term in Taylor expansion of $1/\tau$ around $B_{od}$, assuming $\tau(B_{od})=\infty$.
[21] T. Tamegai *et al.*, Physica C **213**, 33 (1993).
[22] M. Konczykowski *et al.*, Physica C **341**, 1317 (2000).
[23] B. Kalisky, A. Shaulov, and Y. Yeshurun, Proceedings of LT23, Japan, 2002 (unpublished).